



Published in final edited form as:

Cell Rep. 2023 March 28; 42(3): 112274. doi:10.1016/j.celrep.2023.112274.

Latexin regulates sex dimorphism in hematopoiesis via gender-specific differential expression of microRNA 98-3p and thrombospondin 1

Xiaojing Cui¹, Cuiping Zhang¹, Fang Wang¹, Xinghui Zhao¹, Shuxia Wang², Jinpeng Liu³, Daheng He³, Chi Wang³, Feng-Chun Yang^{4,5}, Sheng Tong⁶, Ying Liang^{1,7,*}

¹Department of Toxicology and Cancer Biology, University of Kentucky, Lexington, KY 40536 USA

²Department of Pharmacology and Nutritional Sciences, University of Kentucky, Lexington, KY 40536 USA

³Division of Cancer Biostatistics, Department of Internal Medicine, University of Kentucky, Lexington, KY 40536 USA

⁴Department of Cell Systems & Anatomy, University of Texas Health Science Center at San Antonio, San Antonio, TX 78229, USA

⁵Mays Cancer Center, University of Texas Health Science Center at San Antonio, San Antonio, TX 78229, USA

⁶Department of Bioengineering, University of Kentucky, Lexington, KY 40536, USA

⁷Lead contact

SUMMARY

Hematopoietic stem cells (HSCs) have the ability to self-renew and differentiate to all blood cell types. HSCs and their differentiated progeny show sex/gender differences. The fundamental mechanisms remain largely unexplored. We previously reported that latexin (*Lxn*) deletion increased HSC survival and repopulation capacity in female mice. Here, we find no differences in HSC function and hematopoiesis in *Lxn* knockout (*Lxn*^{-/-}) male mice under physiologic and myelosuppressive conditions. We further find that *Thbs1*, a downstream target gene of *Lxn* in female HSCs, is repressed in male HSCs. Male-specific high expression of microRNA 98-3p (miR98-3p) contributes to *Thbs1* suppression in male HSCs, thus abrogating the functional effect of *Lxn* in male HSCs and hematopoiesis. These findings uncover a regulatory mechanism

This is an open access article under the CC BY-NC-ND license (<http://creativecommons.org/licenses/by-nc-nd/4.0/>).

*Correspondence: ying.liang@uky.edu.

AUTHOR CONTRIBUTIONS

X.C. performed the majority of experiments and wrote the manuscript; C.Z. was involved in *Lxn*^{-/-} mice generation; F.W., F.-C.Y., and S.T. were involved in miRNA and antagomir study; X.Z. was involved in qPCR and western blot experiments; S.W. provided the *Thbs1* mice; J.L., D.H., and C.W. performed RNA-seq analyses and statistical analyses; Y.L. guided the overall project, designed the experiments, and wrote the manuscript.

SUPPLEMENTAL INFORMATION

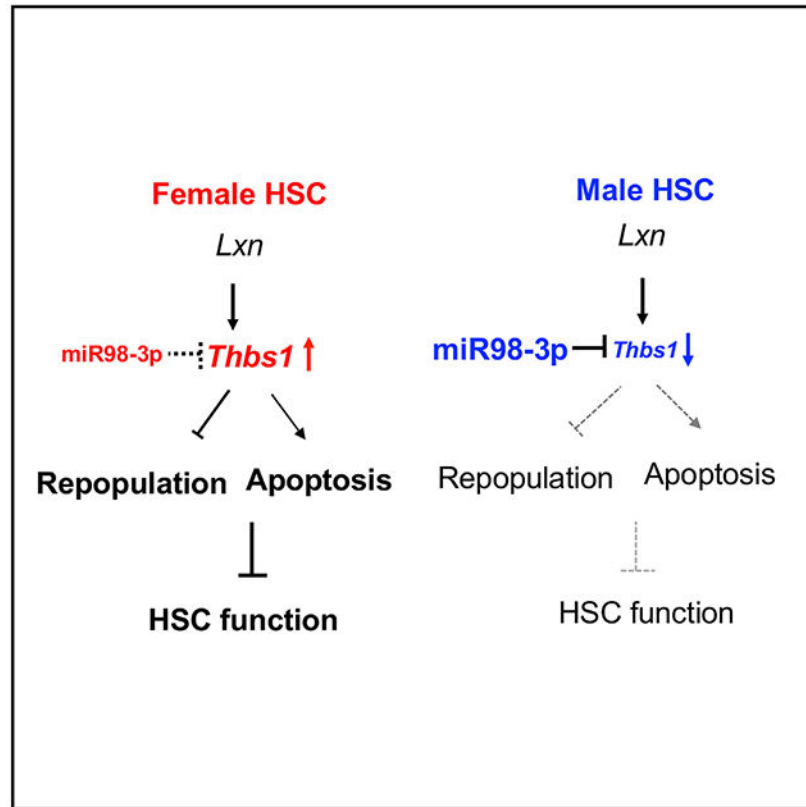
Supplemental information can be found online at <https://doi.org/10.1016/j.celrep.2023.112274>.

DECLARATION OF INTERESTS

These works are related to US patents US 10,604,756 B2; US 9,284,530 B2, and US 2010/0183585 A1. Y.L. is the patent holder.

involving a sex-chromosome-related microRNA and its differential control of *Lxn-Thbs1* signaling in hematopoiesis and shed light on the process underlying sex dimorphism in both normal and malignant hematopoiesis.

Graphical abstract



In brief

In both normal and pathological conditions, blood-forming stem cell activity and the blood system exhibit gender differences. Cui et al. discover that the latexin/microRNA-*Thbs1* signaling pathway contributes to such differences between males and females and is responsible for hematopoiesis sex dimorphism.

INTRODUCTION

Hematopoietic stem cells (HSCs) are a rare population of cells that persist in the bone marrow. HSCs form the entire blood system by their self-renewal capacity and the ability to differentiate into a variety of hematopoietic progenitor cells (HPCs).¹ In the physiologic condition, the number of circulating HPCs in women is lower than in men.² In mice, female HSCs divide more frequently and self-renew more efficiently than male HSCs.³ Women consistently exhibit a lower incidence of hematologic cancers compared with men.⁴ Female pediatric and young adult patients with acute myeloid leukemia (AML) demonstrated increased survival over males.^{5,6} Moreover, female patients with leukemia

showed better recovery from HSC transplantation and less incidence of graft-versus-host disease (GVHD).^{7,8} It is reported that women have higher hematologic toxicity compared with men after the treatment with 5-fluorouracil (5-FU).⁹ Although considerable differences exist between male and female hematopoiesis in both normal and malignant conditions, the underlying mechanisms are not well defined. Estrogen plays a role in the regulation of female hematopoiesis.^{3,10} Gender-specific immune responses exist in which females tend to have a stronger immune reaction.^{11–13} In this study, we found that the HSC regulatory gene latexin (*Lxn*) regulates HSC function and hematopoiesis in a sex-/gender-specific manner and further identified the underlying molecular mechanism.

Our group was the first to report a novel function of *Lxn* in hematopoiesis, in which its expression variation correlates negatively with population HSC number variation.¹⁴ We further generated *Lxn* knockout (*Lxn*^{-/-}) mice and uncovered that *Lxn* deletion *in vivo* enhances HSC survival and regeneration.¹⁵ Our group further reported, for the first time, several novel functions and mechanisms of *Lxn* in the regulation of hematopoiesis, including (1) ribosomal protein subunit 3 (Rps3) is a novel *Lxn*-binding protein,¹⁶ (2) high-mobility group protein 2 (HMGB2) is a novel transcription suppressor of *Lxn* in HSCs,¹⁷ and (3) *Lxn* is involved in hematologic malignancy.¹⁸ *Lxn* is a cytoplasm protein and is the only known endogenous carboxypeptidase A (CPA) inhibitor in mammals.^{19–22} However, we found that its mechanism of function in hematopoietic and lymphoma cell lines is not through the CPA inhibition pathway.¹⁸ Instead, we discovered thrombospondin 1 (*Thbs1*) as a new downstream target of *Lxn*, in which *Lxn* deletion reduces *Thbs1* expression in HSCs, resulting in increased HSC survival and expansion.¹⁵ The function of *Thbs1* in hematopoiesis is largely unknown. It is reported to be involved in the development of human megakaryocyte.²³ It is an important angiogenic regulator that may regulate hematopoiesis as a bone marrow niche-derived extrinsic factor.²⁴

Our discovery of *Lxn-Thbs1* signaling in normal hematopoiesis was made in female mice. Very interestingly, we found in our current study that *Lxn* deletion *in vivo* did not cause any changes of HSC number or function in male mice, which suggests that *Lxn* may function differently for male and female hematopoiesis. We next performed RNA sequencing (RNA-seq) of hematopoietic stem and progenitor cells (HSPCs) from male and female *Lxn*^{-/-} and wild-type (WT) mice and searched for candidate genes with a differential expression in female *Lxn*^{-/-} and WT HSPCs but not in males. *Thbs1* was the top candidate, and its expression was very low in male HSPCs. We further identified a sex-chromosome-specific microRNA that contributes to the low expression of *Thbs1* in male HSPCs, thus abrogating the effect of *Lxn* in male HSCs and hematopoiesis. In conclusion, our study first shows a sex-/gender-specific effect of the *Lxn* gene in the regulation of hematopoiesis. Sex-chromosome-specific microRNA downregulates the expression of the *Lxn* downstream target gene *Thbs1*, thus abrogating the *Lxn* effect in male hematopoiesis.

RESULTS

***Lxn* deletion *in vivo* does not affect the number of blood cells and BM HSPCs in male mice**

In order to understand the regulation of *Lxn* in hematopoiesis in a sex-specific manner, we performed peripheral blood (PB) and bone marrow (BM) analyses in WT and *Lxn*^{-/-} male

and female mice. The counts of white blood cells, lymphocytes, neutrophils, and monocytes showed no difference between male $Lxn^{-/-}$ and WT mice, whereas they were significantly increased in female $Lxn^{-/-}$ mice compared with female WT counterparts (Figures 1A and S1A). We next characterized the BM stem and progenitor populations by using flow cytometry and cell surface markers (Figure 1B). The result showed that the absolute numbers of HSPC-enriched LSK cells, short-term (ST) HSCs, multipotent progenitor (MPP) cells, and common lymphoid progenitor (CLP) cells found no significant difference between male $Lxn^{-/-}$ and WT mice, whereas female $Lxn^{-/-}$ mice had a significant increase in the numbers of these cell populations (Figures 1C–1F and S1B). The hematopoietic changes in $Lxn^{-/-}$ female mice are consistent with our published results.¹⁵ Lxn inactivation expands the HSC population by decreasing the apoptosis in female mice.¹⁵ In male WT and $Lxn^{-/-}$ mice, we analyzed the apoptosis of long-term (LT) HSCs, ST HSCs, MPP cells, and LSK cells by annexin V and 7-AAD (Figure 1H). The data showed that Lxn deletion did not affect the apoptosis of stem and progenitor populations (Figure 1I), which may explain why we did not detect the difference in HSPC populations. Moreover, cell-cycle analysis of each cell population by Ki67 and 7-AAD revealed no difference in male $Lxn^{-/-}$ mice compared with the WT control (Figure S2). Altogether, these data implied that Lxn deletion did not cause any changes in the numbers of blood cells and BM HSPCs in males and that Lxn functions differently between males and females in the regulation of HSPCs.

Deletion of Lxn *in vivo* in male mice does not change the clonogenic and repopulation capacity of BM cells

We further evaluated the number of clonogenic progenitor and stem cells by using colony-forming cell (CFC) assay and cobblestone area-forming cell (CAFC) assay. The results showed that the numbers of CFCs (progenitor) and CAFCs on day 35 (LT HSCs) did not change in $Lxn^{-/-}$ male mice (Figures 2A and 2B). To determine the regeneration function of male $Lxn^{-/-}$ BM cells, we performed a competitive transplantation assay (Figure 2C). Equal numbers (1×10^6) of the donor (male WT or $Lxn^{-/-}$; CD45.2) and competitor (CD45.1 male) BM cells were transplanted into lethally irradiated male CD45.1 recipient mice. Blood and BM chimerism was analyzed at different time points post-transplantation. The results showed that $Lxn^{-/-}$ -derived PB leukocytes, including the circulating myeloid, B, and T cells, showed no significant difference from the WT donor from 4 to 16 weeks post-transplantation (Figures 2D and 2E). For the BM chimerism analyses, the percentages of BM LSK cells, LT HSCs, ST HSCs, and MPP cells that were regenerated from $Lxn^{-/-}$ male BM cells showed no significant difference from those of WT male cells (Figures 3F–3I), suggesting that Lxn deletion in male mice does not affect the repopulation capacity of BM cells. We performed a similar transplantation in the female recipients, and similar results were observed, that is, no difference in the chimerism of PB and BM in male WT and $Lxn^{-/-}$ engrafted cells (Figure S3). These findings are different from female $Lxn^{-/-}$ BM cells in which we showed an increased repopulation capacity.¹⁵ We previously reported that Lxn deletion can stimulate hematopoietic recovery from 5-FU-induced myelosuppression in female mice.¹⁵ Although we did not detect any steady-state hematopoietic changes in $Lxn^{-/-}$ male mice, we wanted to examine whether a stressed condition would impact that outcome. We treated male $Lxn^{-/-}$ and WT mice with 5-FU and monitored dynamic changes of blood white blood cells, BM cellularity, and LSK cells for 2 weeks. Not surprisingly, no

difference in the recovery of these populations between *Lxn*^{-/-} and WT mice was observed (Figures 2J–2L). Similarly, we did not detect any difference in apoptosis of LSK cells (Figure 2M). The results suggest that *Lxn* deletion in male mice also has no effect on stress by 5-FU-induced myelosuppression.

***Thbs1* suppression in male HSCs contributes to *Lxn*-mediated gender-specific regulation of hematopoiesis**

We next investigated the molecular mechanism underlying gender-specific regulation of hematopoiesis by *Lxn*. RNA-seq was performed on LSK cells that were isolated from male WT, male *Lxn*^{-/-}, female WT, and female *Lxn*^{-/-} mice. We compared the male WT group with the female WT group and found that 4,018 genes were differentially expressed. We ranked the genes based on the fold changes and listed the top 50 genes (Figure 3A). We found that *Thbs1*, a previously identified downstream target of *Lxn*, is among them. Its expression was decreased in female *Lxn*^{-/-} LSK cells (compared with female WT cells) but was unchanged in the male comparison group. We further confirmed the sequencing result by quantitative PCR (Figure 3B) and western blot (Figure 3C). Very interestingly, the *Thbs1* mRNA and protein expression levels were very low in male LSK cells regardless of whether *Lxn* was depleted or not, which suggests that low expression of *Thbs1* in male cells may abrogate the effect of *Lxn* in male hematopoiesis. We previously reported that the decreased expression of *Thbs1* increased *Lxn*^{-/-} HSC survival in females by decreasing the active caspase-3 level. In male *Lxn*^{-/-} HSCs, caspase-3 in LSK cells by flow cytometry and western blot showed no change (Figures 3D–3F). These results further support the hypothesis that *Thbs1* might be involved in gender-specific hematopoiesis regulated by *Lxn*. To test that idea, we measured the LSK number in male WT, male *Thbs1*^{+/-}, female WT, and female *Thbs1*^{+/-} mice. We found that there was no significant difference in LSK number between male WT and male *Thbs1*^{+/-} mice, but as reported previously, female *Thbs1*^{+/-} mice showed a higher LSK number than female WT mice (Figures 3G and 3H). Thus, the gender-dependent regulation of HSCs and hematopoiesis by *Lxn* is attributable to the low expression of *Thbs1* in male mice.

miR98-3p directly binds to *Thbs1* and inhibits its expression *in vitro*

To explore why the expression of *Thbs1* is dramatically lower in male HSPCs, we first identified the methylation levels of the CpG islands in the promoter region of *Thbs1* in male and female lineage-negative populations (Lin⁻) by using bisulfite sequencing. We found there was no difference in the methylation level at the *Thbs1* promoter between male and female HSPCs (Figure S4). MicroRNA (miRNA) was reported to regulate the *Thbs1* mRNA level^{25–27} by binding to the 3' untranslated region (UTR) and inducing mRNA degradation^{28,29}; the higher the miRNA expression, the lower the *Thbs1* expression. We thus hypothesized that sex-chromosome-specific differential expression of miRNA could contribute to the low expression of *Thbs1* in male HSPCs. We used the web tool (miRDB [MicroRNA Target Prediction Database]) to predict miRNAs that could potentially bind to the 3' UTR of *Thbs1* mRNA. We then chose the candidate miRNAs that were located in the sex chromosome and identified 11 miRNAs (Figure 4A). We measured the expression of these miRNAs by quantitative PCR in male and female *Lxn*^{-/-} and WT LSK cells and selected the miRNA with high expression in male cells and low expression in female

cells (opposite to *Thbs1* expression). miR98-3p is the only candidate gene that met this criterion. We next determined whether miR98-3p inhibits *Thbs1* expression. We transfected a miR98-3p mimic and a control mimic into the 3T3 cell and checked the expression of miR98-3p and *Thbs1*. The mimic significantly increased miR98-3p expression (Figure 4B) and decreased *Thbs1* expression (Figure 4C), which suggests that miR98-3p inhibits the *Thbs1* mRNA level. To verify the direct binding of miR98-3p to *Thbs1* 3'UTR, we performed a luciferase reporter analysis. We used an miR98 precursor (pre-miR98) to ensure a stable, high expression of miR98-3p (Figure 4D) and cloned it into a pcDNA3.1 vector. Next, we cloned the *Thbs1*-3' UTR that contained the miR-98-3p binding (seed) region into a PGL3 vector (*Thbs1*-3' UTR-WT). The *Thbs1*-3' UTR-mutant clone (*Thbs1*-3' UTR-mut; Figure 4E) had the mutated seed region, which was used as the non-binding negative control. As shown in Figure 4F, the relative luciferase activity of *Thbs1*-3' UTR-WT was significantly reduced by the pre-miR98 (column 1 and 2), whereas pre-miR98 showed no effect in either pcDNA3.1 control or *Thbs1*-3' UTR-mut negative controls (column 3 and 4). These data demonstrate that the miR98-3p can directly bind to the 3' UTR region of *Thbs1* and contribute to the downregulation of *Thbs1* mRNA.

miR98-3p increases the number of clonogenic HSPCs by decreasing *Thbs1* level

To further verify the effect of miR98-3p on *Thbs1* level and on the function of primary HSPCs, we overexpressed the miR98-3p mimic in female WT LSK cells (high *Thbs1* expression) and determined its effect on the *Thbs1* level and clonogenic HSPC number. We first confirmed the increased expression of miR98-3p (Figure 5A). With enforced expression of miR98-3p, we found that *Thbs1* mRNA and protein levels both decreased (Figures 5B and 5C), suggesting that miR98-3p downregulates *Thbs1* expression in primary HSPCs. We further evaluated the functional effect of miR98-3p on HSPCs and found that it increased the number of CAFCs on day 21, which represent HSPCs (Figure 5D). We next transplanted the miR98-3p mimic (or control miRAN [miR])-treated LSK cells into the lethally irradiated CD45.1 recipient mice and found that miR98-3p treatment significantly increased the engraftment of PB cells at different time points post-transplant compared with the control group (Figure 5E). The result strongly supports that miR98-3p represses *Thbs1* expression and consequently increases HSPC clonogenic and repopulation function.

Our published work also showed that *Lxn* deletion downregulates *Thbs1*.¹⁵ How these two mechanisms (miR98-3p and *Lxn*) independently or coordinately regulate *Thbs1* in males and females is not clear. To answer this question, we first determined the mRNA and protein expression of *Lxn* and *Thbs1* in PB white blood cells (WBCs), BM Lin⁻, and LSK cells along the hematopoietic hierarchy. The result showed that *Lxn* mRNA and protein expression increased in concert with the content of primitive hematopoietic cells in which LSK cells had the highest expression (Figures 5F and 5G). This result is consistent with our previous report.¹⁵ More importantly, *Lxn* expression was similar between male and female cells. Very interestingly, the expression pattern of *Thbs1* along the hematopoietic hierarchy is opposite to *Lxn* in both differentiation and sex-specific manner, that is, *Thbs1* expression was very low in male LSK cells (Figures 5H and 5I). This result indicates that *Lxn* and miR98-3p may coordinately contribute to the regulation of *Thbs1* but in a sex-dependent manner. To further dissect these two pathways, we treated male and female *Lxn*^{-/-} LSK

cells with mir98-3p antagomir and examined the *Thbs1* expression. We first confirmed the decreased expression of mir98-3p by real-time PCR (Figure 5J). We then examined the *Thbs1* protein level, and as expected, its expression was significantly increased in male LSK cells but not in female cells (Figure 5K). This result strongly suggests that mir98-3p regulates the *Thbs1* expression in a sex-dependent manner and that it plays a major role in male HSPCs. In female HSPCs, low miR98-3p expression causes high *Thbs1* expression, resulting in a low HSPC number. In contrast, miR98-3p expression is very high in male HSPCs, leading to a very low level of *Thbs1*, which abrogates the effect of *Lxn* on male HSPCs (Figure 5L).

DISCUSSION

Gender difference exists in HSPCs under normal or stress conditions, as well as in blood disorder disease. However, there are few studies on the sex/gender difference in hematopoiesis, and the underlying molecular mechanisms remain largely unknown. In this study, we revealed a novel role of *Lxn* in regulating hematopoiesis in a sex-/gender-specific manner and identified that sex-chromosome-dependent differential expression of a miRNA contributes to this difference.

In our published data, *Lxn* acts endogenously in HSCs to negatively regulate HSCs population size by enhancing apoptosis and decreasing self-renewal. *Lxn* deletion prompts hematopoietic recovery after 5-FU chemotherapy.¹⁵ Furthermore, *Lxn* deficiency decreases the expression of active caspase-3 by downregulating *Thbs1*.¹⁵ All these data were collected from female mice. However, in the current work, we found that *Lxn* deletion caused no changes in apoptosis, proliferation, and regeneration of HSCs in male mice for both the steady-state and 5-FU-induced stress conditions. Moreover, it did not affect HSC differentiation, thus blood cell counts and lineage differentiation were not altered in male *Lxn*^{-/-} mice. Taken together, the data suggest that *Lxn* regulates HSCs and hematopoiesis in a sex-/gender-dependent manner.

Sex-/gender-dependent regulatory mechanisms could contribute to differences in reproductive organs, hormones, and/or sex chromosomes between male and female. Sex hormones, such as estrogen and the luteinizing hormone,³⁰⁻³² have been shown to contribute to the sexual dimorphism in hematopoiesis. Here, we reported a novel mechanism involved in sex-chromosome-related miRNA level and its effect on the *Lxn-Thbs1* signaling and sexual dimorphism. *Thbs1* is a specific downstream target of *Lxn*, and the decreased level of *Thbs1* mediates a functional effect of *Lxn* on HSCs in female mice. However, we found that *Thbs1* expression was dramatically lower in male HSPCs compared with female cells. It may be that the expression of *Thbs1* is too low to be regulated by *Lxn* in male mice, which would result in no *Lxn* effect on hematopoiesis in male mice. The low expression of *Thbs1* was not due to promoter hypermethylation but rather due to sex-chromosome-dependent differential expression of miRNA. Our work identified miR98-3p as the factor that contributes to the lower expression of *Thbs1* in male HSPC by showing that (1) miR98-3p is highly expressed in male HSPCs; (2) the high expression of miR98-3p in male HSPCs is correlated with lower expression of *Thbs1*; (3) miR98-3p directly binds to the 3' UTR of *Thbs1* and directs it to degradation, thus resulting in its lower expression; and

(4) enforced miR98-3p expression causes *Thbs1* downregulation, resulting in an increased HSPC number. These data strongly support a role of miR98-3p in regulation of *Thbs1* expression and HSPC function. Thus, miR98-3p contributes to the low expression of *Thbs1* in male HSPCs, thus abrogating the effect of *Lxn* in male HSCs and hematopoiesis.

The mechanism of how *Lxn* and (or) miR98-3p regulate *Thbs1* in HSPCs is completely unknown. Our published work showed that *Lxn* binds to an Rps3¹⁶ and that *Lxn* downregulates *Thbs1* mRNA and protein expression.¹⁵ Rps3 has been reported to specifically bind to the p65 subunit of the nuclear factor κ B (NF- κ B) complex.^{33,34} We hypothesize that *Lxn* deficiency could promote nuclear translocation of the NF- κ B complex and enhance its transcription activity. miR98-3p is one of the transcription targets of NF- κ B. Thus, *Lxn*/NF- κ B/miR98-3p/*Thbs1* could be the potential signaling pathway. However, it is also possible that both *Lxn* and miR98-3p coordinately contribute to the regulation of *Thbs1* but in a sex-dependent manner. As shown in Figure 3, in male HSPCs, miR98-3p may be a major regulator for *Thbs1* expression because *Thbs1* protein expression is very low in both WT and *Lxn*^{-/-} HSPCs. In female HSPCs, *Lxn* may play a more important role in regulating *Thbs1* expression because the *Thbs1* protein level was significantly decreased in female *Lxn*^{-/-} HSPCs in which miR98-3p expression is lower. In addition, we found that *Lxn* expression did not show a gender difference along the hematopoietic hierarchy, whereas *Thbs1* showed a dramatic sex difference. Moreover, we treated *Lxn*^{-/-} male and female LSK cells with miR98-3p antagomir to determine the sole effect of miR98-3p on *Thbs1* expression and found that *Thbs1* expression was significantly increased in male LSK cells but not in female cells. All these results strongly suggest that differential expression of sex-chromosome-specific miR98-3p contributes to sex-dependent expression of *Thbs1*.

These studies uncovered that the sex/gender differences in *Lxn* function for HSC regulation under normal conditions. These findings may provide general mechanistic insights about sexual dimorphism in HSC function and hematopoiesis. By defining the role of *Lxn* in regulating male and female HSCs under normal conditions, it would be interesting to determine whether *Lxn* expression changes correlate with hematologic recovery in male and female patients with cancer after cancer therapy in the future.

Limitations of the study

This study was performed in the physiological condition and 5-FU-induced myelosuppression. It would be interesting to investigate whether *Lxn* shows gender-specific regulation of HSCs and hematopoiesis under other types of stresses, such as radiation, aging, and other chemotherapeutic drug-induced myelosuppression. It would be also interesting to understand the signaling *Lxn/miRNA-983p-Thbs1* pathway in sex dimorphism in hematologic malignancy.

STAR★METHODS

RESOURCE AVAILABILITY

Lead contact—Further information and requests for resources and reagents should be directed to and will be fulfilled by the lead contact, Ying Liang (ying.liang@uky.edu).

Materials availability—All materials will be available upon request to the lead contact.

Data and code availability

- The RNAseq data is in the GEO database: GSE213283.
- This paper does not report original code.
- Any additional information required to reanalyze the data reported in this work paper is available from the lead contact upon request.

EXPERIMENTAL MODEL AND SUBJECT DETAILS

Animals—C57BL/6 mice and B6.SJL/BoyJ (CD45.1) recipient mice were purchased from The Jackson Laboratory. Our group has reported the generation and validation of *Lxn* constitutive knockout mice (*Lxn*^{-/-}) previously.¹⁵ All mice used were male and 8–16 weeks old. Mice were housed at the University of Kentucky animal facilities following NIH mandated guidelines for animal welfare and with IACUC approval. Complete blood count was performed on a Hemavet 950 (Drew Scientific). Mice were exposed to lethal (9Gy) dose of total body irradiation in a Mark 1 irradiator (137 Cesium) (J.L. SHEPHERD & ASSOCIATES, Glendale, CA) at a rate of 1.0 Gy/min with attenuator. Male mice were irradiated on a rotating platform. Male mice were treated with 5-FU (150 mg/kg body weight) by intraperitoneal injection.

Cell culture—293T and 3T3 cell lines were stored in own lab and cultured in DMEM medium supplemented with 10% FBS. All cells were cultured at 37°C in humidified 5% CO₂ atmosphere.

METHOD DETAILS

Flow cytometry—Whole bone marrow cells (BM) from the femur of 8-16 weeks mice were isolated. For LT-HSC, ST-HSC and MPP, BM cells were stained for lineage, sca-1, ckit, CD135 and CD34. For GMP, CMP and MEP progenitor cells, BM cells were stained for lineage, ckit, FcγR and CD34. CLP cells were defined with LSK markers, CD127 and CD135. PB lineage chimerism staining was CD45.1, CD45.2, CD90.2, Mac-1, Gr-1, and B220¹⁵. For the cell apoptosis analysis, BM cells were stained with Annexin V and 7-AAD (7-aminoactinomycin D).¹⁷ Cell cycle analysis were performed by staining Ki-67 and 7-AAD. Flow cytometry was performed and analyzed on the Cytometers BD LSR II.

In vitro colony assay—CFC assay (colony forming assay): bone marrow cells, isolated from the femur, were plated to the 35mm² dish and cultured in the MethoCult medium (STEMCELL Technologies). Each dish was seeded with 1 × 10⁴ cells. The colony formation was assessed on day 7 and 14³⁵.

Cobblestone area-forming cell (CAFC) assay were performed as described previously.¹⁴ Bone marrow cells or cultured LSK cells were seeds in 96-wells plates with full confluence of FBMD1 cells. The bone marrow cells were seeds at a dose of 81000, 27000, 9000, 3000, 1000, and 333. The cultured LSK cells were seeds at a dose of 2666.7, 888.9, 296.3, 98.8, 33, and 11. We evaluated 20 replicate wells per dose. The cobblestones formation was

assessed on day 7, 14, 21, 28, and 35. Colonies appeared later in time derived from more primitive cells.¹⁴ CAFC frequencies were calculated and analyzed by using L-CaLc limiting dilution analysis software (STEMCELL Technologies).

Competitive transplantation assay— 1×10^6 donor cells from male *Lxn*^{-/-} or WT BM (CD45.2) were mixed with the equal number of competitor BM cells (male B6.SJL/BoyJ) and retro-orbitally injected into lethally irradiated recipient mice (male B6.SJL/BoyJ). Percentages of donor cells (CD45.2) in PB cells were determined at 4, 8, 12, 16 weeks. Percentages of donor cells in BM were determined at 16 weeks post-transplantation.¹⁴

Western Blot—The total proteins of cells were isolate by RIPA buffer (Sigma) with the protease inhibitor cocktail (CST). Lysates were cleared by centrifugation, then denatured with heat and reducing agents. The samples were separated on a 10% Bis-Tris gel (Novex) and electro-transferred to PVDF membranes (Millipore). Subsequently, the membranes were blocked and incubated with specific antibodies. Latexin antibody was bought from Proteintech, Thbs1 antibody was bought from Santa Cruz, actin antibody were bought from Sigma. The membrane with the primary antibody was incubated in 4°C overnight. The secondary anti-rabbit or anti-mouse IgG, HRP-linked antibodies (CST) were incubated for 1h at room temperature. Chemiluminescence detected by exposing the membrane to X-ray film or exposed in Azure Biosystems C600.

mRNA quantification—LSK cells were isolated by fluorescence cell sorting and were used to extract the cDNA as described previously. Total RNA was isolated by using the mirVana miRNA isolation kit (Invitrogen). cDNA reverse transcription were performed by using the high-capacity cDNA reverse transcription kit (Applied Biosystems). Quantitative real-time PCR was performed with the commercially available Taqman probe for *Thbs1*, *Lxn*, and *Gapdh* by using the TaqMan Universal PCR Master Mix (Applied Biosystems) in ABI StepOnePlus Real-Time PCR (Applied Biosystems).

miRNA qPCR—LSK cells were isolated from bone marrow by fluorescence cell sorting and were used to extract the total RNA by using mirVana miRNA isolation kit (Invitrogen). cDNA extraction and miRNA qPCR were conducted by following the protocol of all-in-one miRNA qRT-PCR Detection Kits (GeneCopoeia). The miRNA primers were designed by following the tail reactive rule. The sequences of primers used in this study are miR98-3p: AGCGAGGCCTATACAACCTACTACT; miR98-5p: AAGCGACCTGAGGTAGTAAGTTGTA; U6: CTCGCTTCGGCAGCACACA; miR201-5p: AACCGGTACTCAGTAAGGCATTG; miR-6382: AACAGTGTGGAATGTAAAGAGAGCA; miR-450a-2-3p: AACAAATATTGGGGATGCTTTGCATT; miR-18b-5p: AACACGCTAAGGTGCATCTAGTG; miR-384-3p: AACGGCATTCTAGAAATTGTTTAC; miR-105: AACAGTGCCAAGTGCTCAGATG; miR-883a-3p: AACAGATAACTGCAACAGCTCTCAG; miR-883b-3p: AACCACTTAACTGCAACATCTCTCA; miR-325-3p: AACCATGTTTATTGAGCACCTCCT.

MiR98-3p manipulation in LSK cells—1) Overexpression of MiR98-3p mimic in LSK cells: LSK cells were sorted by flow cytometry. The LSK cells were recovered and incubated overnight, then transfected with control or miR98-3p mimics by using lipofectamine 3000. Additionally, after 36h incubation, LSK cells were collected and transfected with control or miR98-3p mimics. CAFC assay, western-blot, or qPCR were conducted as described above. 2) Inhibition of miRNA-98-3p using antagonist in LSK cells. To achieve the loss-of-function of miRNA-98-3p, the antagomir of mir-98 (MNM03274) was designed and synthesized with chemical modification by Applied Biological Materials (abm) Inc. Flow cytometry sorted LSK cells from male and female *Lxn*^{-/-} mice were recovered with cytokines including 100 ng/mL FMS-like tyrosine kinase-3 ligand, 50 ng/mL mouse stem cell factor, 10 ng/mL interleukin-3, and 10 ng/mL IL-6 in StemSpan SFEM (STEMCELL Technologies) for 2 h at 37°, 5% CO₂. Then cells were continued to be cultured and treated with or without mir-98 antagomir (500nM) for 24 h. Cells were then collected for microRNA and protein isolation. MicroRNA was isolated by using RNeasy Micro Kit (Qiagen); cDNA synthesis and qPCR were performed with All-in-One miRNA qRT-PCR Detection Kit 2.0 (Genecopoeia). Protein expression of THBS1 was determined by Western blot analysis, as described above.¹⁵

Dual-luciferase reporter assays—To perform the luciferase experiment, we constructed pre-miR98 plasmid, pGL3-*Thbs1-3'* UTR-wt plasmid, and pGL3-*Thbs1-3'* UTR-mut plasmid. To construct the pre-miR98 plasmid, we cloned the miR98 sequence into pcDNA3.1 plasmid, and the pcDNA3.1 vector was used as a sham control. The pGL3-*Thbs1-3'* UTR-wt plasmid was created by cloning the specific miR98-3p binding sequence (seed region) into the Xba I site of pGL3 reporter vector. The pGL3-*Thbs1-3'* UTR-mut plasmid (which was used as a negative control) was constructed by inserting the muted seeds region into pGL3 vector. pRL-null was used as the internal control vector to balance transfection efficiency. The 293T cells were transfected by 4 groups of plasmids: 1) pGL3-*Thbs1-3'* UTR-WT and pcDNA3.1 (Figure 4F 1st column); 2) pGL3-*Thbs1-3'* UTR-WT and pcDNA3.1-pre-miR98 (second column); 3) pGL3-*Thbs1-3'* UTR-mut and pcDNA3.1 (3rd column); and 4) pGL3-*Thbs1-3'* UTR-mut and pcDNA3.1- pre-miR98 ((4th column). After incubation 48h in 37°C, the luciferase activity was detected by using Dual-Glo Luciferase Assay System (Promega). The sequences of primers used in this study are Pre-miR98 forward primer (5' to 3'): CGGGATCCCATTACATACATATACTTCTCATTCCCTTCT, reverse primer: CGGAATTCGTATGAACCAACATGCCTTGC; pGL3-*Thbs1-3'* UTR-wt forward primer: GCTCTAGAGCCATTTTTATCCATTTTACATTCTAAAGCAGTGTAACCTTGATAT, reverse primer: GCTCTAGAGCTACATAAGAAACAGTAATATACAAGTTACTGCTTTAGAATGT; pGL3-*Thbs1-3'* UTR-mut forward primer: GCTCTAGAGCCATTTTTATCCATTTTACATTCTAAAGCAGTGTAACCTTTTTTTT, reverse primer: GCTCTAGAGCTACATAAGAAACAGTAAAAAAAAGTTACTGCTTTAGAATGT.

Bisulfite sequencing—To explore the methylation modification of *Thbs1* promoter, we obtained the nucleotide sequence of *Thbs1* promoter region from Ensembl database

with the ID number ENSMUSG00000040152. A 260bp region and a 147bp region of CpG island in Thbs1 promoter was predicted in website “<http://www.urogene.org/cgi-bin/methprimer/methprimer.cgi>”. The 260bp region located at chromosome 2: 117,942,070–117,942,330, with 19 CpG dinucleotides. The 147bp region located at chromosome 2: 117,942,405–117,942,552, with 12 CpG dinucleotides. We isolated the Lineage negative population by using Lineage Depletion Kit (Miltenyi Biotec). Genomic DNAs from Lineage negative cells were isolated by using Genomic DNA extraction Kit (ThermoFisher) and converted the unmethylated cytosines to uracils by using Epiect Bisulfite Kits (Qiagen). To amplify the CpG island region, we use Platinum II Taq Hot-Start DNA Polymerase (ThermoFisher) and follow the commercial protocol to conduct the PCR assay. For 260bp region, the forward primer is TTTTAGGTGGTTTTTAAAGAAGTAT, and the reverse primer is TAAAAAAACAAAAACAAAAAAA. For 147bp region, the forward primer is TTTAGTTAAGTTAGTTATTGTTTGGAGTTA, and the reverse primer is CTAATCATCTACAACCTAAAACCTTTAAAT. Then the amplified fragments were ligated to pCR 2.1-TOPO TA vector and conducted transformation. Three positive colonies were selected to extract plasmid and sequenced.

RNA sequencing and analysis—LSK cells were isolated from bone marrow of male C57BL/6 mice, female C57BL/6 mice, male *Lxn*^{-/-} mice, and female *Lxn*^{-/-} mice. Total RNA was isolated by using NEBNext Ultra RNA Library Prep Kit. Directional polyA RNA-seq was performed by the Genomics, Epigenomics and Sequencing Core at the University of Cincinnati using established protocols as previously mentioned (PMID: 31120332 and 31420676). Briefly, the quality of total RNA was QC analyzed by Bioanalyzer (Agilent, Santa Clara, CA). To isolate polyA RNA for library preparation, NEBNext Poly(A) mRNA Magnetic Isolation Module (New England BioLabs, Ipswich, MA) was used with 400 ng good quality total RNA as input. The polyA RNA was enriched using SMARTer Apollo automated NGS library prep system (Takara Bio USA, Mountain View, CA). Next, NEBNext Ultra II Directional RNA Library Prep kit (New England BioLabs) was used for library preparation under PCR cycle number of 9. After library QC and quantification via real-time qPCR (NEBNext Library Quant Kit, New England BioLabs), individually indexed libraries were proportionally pooled and sequenced using NextSeq 550 sequencer (Illumina, San Diego, CA) under the sequencing setting of single read 1 × 85 bp. Sequencing reads were trimmed and filtered using Trim Galore (https://www.bioinformatics.babraham.ac.uk/projects/trim_galore/) to remove adapters and low-quality reads. Reads from mouse samples were mapped to Ensembl GRCm38 transcripts annotation using RSEM.³⁶ RSEM results normalization and differential expression analysis were performed using the R package edgeR.³⁷ Significantly up/downregulated genes were determined as q-value <0.05. The gene set enrichment analysis was performed using GSEA software.³⁸

QUANTIFICATION AND STATISTICAL ANALYSIS

The Markey Cancer Center Biostatistics & Bioinformatics Shared Resource Facility was consulted for the experimental design and statistical analysis. Data were examined for homogeneity of variances (F test), then analyzed by a two-tailed, unpaired Student’s t-test. Statistical analyses were performed using GraphPad Prism Software version 7.0 to 9.0.

Results shown represent mean \pm SD. Differences were considered significant at $p < 0.05$. * $p < 0.05$, ** $p < 0.01$, *** $p < 0.001$ and **** $p < 0.0001$.

Supplementary Material

Refer to Web version on PubMed Central for supplementary material.

ACKNOWLEDGMENTS

The authors are supported by the National Institutes of Health under awards R01HL124015 (Y.L.) and R21HL140213 (Y.L.) and the Markey Cancer Center's Flow Cytometry and Immune Monitoring Core and Biostatistics and Bioinformatics Shared Resource Facilities (P30CA177558). We thank the Markey Cancer Center's Research Communications Office for editing and graphics support.

REFERENCES

1. Eaves CJ (2015). Hematopoietic stem cells: concepts, definitions, and the new reality. *Blood* 125, 2605–2613. 10.1182/blood-2014-12-570200. [PubMed: 25762175]
2. Topel ML, Hayek SS, Ko YA, Sandesara PB, Samman Tahhan A, Hesaroieh I, Mahar E, Martin GS, Waller EK, and Quyyumi AA (2017). Sex differences in circulating progenitor cells. *J. Am. Heart Assoc.* 6, e006245. 10.1161/jaha.117.006245. [PubMed: 28974500]
3. Nakada D, Oguro H, Levi BP, Ryan N, Kitano A, Saitoh Y, Takeichi M, Wendt GR, and Morrison SJ (2014). Oestrogen increases haematopoietic stem-cell self-renewal in females and during pregnancy. *Nature* 505, 555–558. 10.1038/nature12932. [PubMed: 24451543]
4. Cronin KA, Lake AJ, Scott S, Sherman RL, Noone AM, Howlader N, Henley SJ, Anderson RN, Firth AU, Ma J, et al. (2018). Annual report to the nation on the status of cancer, part I: national cancer statistics. *Cancer* 124, 2785–2800. 10.1002/cncr.31551. [PubMed: 29786848]
5. Hossain MJ, and Xie L (2015). Sex disparity in childhood and young adult acute myeloid leukemia (AML) survival: evidence from US population data. *Cancer Epidemiol.* 39, 892–900. 10.1016/j.canep.2015.10.020. [PubMed: 26520618]
6. Juliusson G, and Hough R (2016). Leukemia. *Prog. Tumor Res* 43, 87–100. 10.1159/000447076. [PubMed: 27595359]
7. Gratwohl A, Ruiz de Elvira C, Gratwohl M, Greinix HT, and Duarte R; Graft-versus-Host Disease Subcommittee of the Complications and Quality of Life Working Party of the European Society for Blood and Marrow Transplantation (2016). Gender and graft-versus-host disease after hematopoietic stem cell transplantation. *Biol. Blood Marrow Transplant* 22, 1145–1146. 10.1016/j.bbmt.2016.03.020. [PubMed: 27032302]
8. Kim HT, Zhang MJ, Woolfrey AE, St Martin A, Chen J, Saber W, Perales MA, Armand P, and Eapen M (2016). Donor and recipient sex in allogeneic stem cell transplantation: what really matters. *Haematologica* 101, 1260–1266. 10.3324/haematol.2016.147645. [PubMed: 27354023]
9. Chansky K, Benedetti J, and Macdonald JS (2005). Differences in toxicity between men and women treated with 5-fluorouracil therapy for colorectal carcinoma. *Cancer* 103, 1165–1171. 10.1002/cncr.20878. [PubMed: 15693031]
10. Heo HR, Chen L, An B, Kim KS, Ji J, and Hong SH (2015). Hormonal regulation of hematopoietic stem cells and their niche: a focus on estrogen. *Int. J. Stem Cells* 8, 18–23. 10.15283/ijsc.2015.8.1.18. [PubMed: 26019751]
11. Klein SL, and Flanagan KL (2016). Sex differences in immune responses. *Nat. Rev. Immunol.* 16, 626–638. 10.1038/nri.2016.90. [PubMed: 27546235]
12. Ersvaer E, Liseth K, Skavland J, Gjertsen BT, and Bruserud Ø (2010). Intensive chemotherapy for acute myeloid leukemia differentially affects circulating TC1, TH1, TH17 and TREG cells. *BMC Immunol.* 11, 38. 10.1186/1471-2172-11-38. [PubMed: 20618967]
13. Ben-Batalla I, Vargas-Delgado ME, Meier L, and Loges S (2019). Sexual dimorphism in solid and hematological malignancies. *Semin. Immunopathol.* 41, 251–263. 10.1007/s00281-018-0724-7. [PubMed: 30361802]

14. Liang Y, Jansen M, Aronow B, Geiger H, and Van Zant G (2007). The quantitative trait gene latexin influences the size of the hematopoietic stem cell population in mice. *Nat. Genet* 39, 178–188. 10.1038/ng1938. [PubMed: 17220891]
15. Liu Y, Zhang C, Li Z, Wang C, Jia J, Gao T, Hildebrandt G, Zhou D, Bondada S, Ji P, et al. (2017). Latexin inactivation enhances survival and long-term engraftment of hematopoietic stem cells and expands the entire hematopoietic system in mice. *Stem Cell Rep.* 8, 991–1004. 10.1016/j.stemcr.2017.02.009.
16. You Y, Wen R, Pathak R, Li A, Li W, St Clair D, Hauer-Jensen M, Zhou D, and Liang Y (2014). Latexin sensitizes leukemogenic cells to gamma-irradiation-induced cell-cycle arrest and cell death through Rps3 pathway. *Cell Death Dis.* 5, e1493. 10.1038/cddis.2014.443. [PubMed: 25341047]
17. Zhang C, Fondufe-Mittendorf YN, Wang C, Chen J, Cheng Q, Zhou D, Zheng Y, Geiger H, and Liang Y (2020). Latexin regulation by HMGB2 is required for hematopoietic stem cell maintenance. *Haematologica* 105, 573–584. 10.3324/haematol.2018.207092. [PubMed: 31171637]
18. Liu Y, Howard D, Rector K, Swiderski C, Brandon J, Schook L, Mehta J, Bryson JS, Bondada S, and Liang Y (2012). Latexin is down-regulated in hematopoietic malignancies and restoration of expression inhibits lymphoma growth. *PLoS One* 7, e44979. 10.1371/journal.pone.0044979. [PubMed: 23028717]
19. Normant E, Martres MP, Schwartz JC, and Gros C (1995). Purification, cDNA cloning, functional expression, and characterization of a 26-kDa endogenous mammalian carboxypeptidase inhibitor. *Proc. Natl. Acad. Sci. USA* 92, 12225–12229. [PubMed: 8618874]
20. Uratani Y, Takiguchi-Hayashi K, Miyasaka N, Sato M, Jin M, and Arimatsu Y (2000). Latexin, a carboxypeptidase A inhibitor, is expressed in rat peritoneal mast cells and is associated with granular structures distinct from secretory granules and lysosomes. *Biochem. J.* 346, 817–826. [PubMed: 10698712]
21. García-Castellanos R, Bonet-Figueroa R, Pallarès I, Ventura S, Avilés FX, Vendrell J, and Gomis-Rüth FX (2005). Detailed molecular comparison between the inhibition mode of A/B-type carboxypeptidases in the zymogen state and by the endogenous inhibitor latexin. *Cell. Mol. Life Sci.* 62, 1996–2014. 10.1007/s00018-005-5174-4. [PubMed: 16091843]
22. Pallarès I, Bonet R, García-Castellanos R, Ventura S, Avilés FX, Vendrell J, and Gomis-Rüth FX (2005). Structure of human carboxypeptidase A4 with its endogenous protein inhibitor, latexin. *Proc. Natl. Acad. Sci. USA* 102, 3978–3983. 10.1073/pnas.0500678102. [PubMed: 15738388]
23. Wang H, He J, Xu C, Chen X, Yang H, Shi S, Liu C, Zeng Y, Wu D, Bai Z, et al. (2021). Decoding human megakaryocyte development. *Cell Stem Cell* 28, 535–549.e8. 10.1016/j.stem.2020.11.006. [PubMed: 33340451]
24. Kopp HG, Hooper AT, Broekman MJ, Avecilla ST, Petit I, Luo M, Milde T, Ramos CA, Zhang F, Kopp T, et al. (2006). Thrombospondins deployed by thrombopoietic cells determine angiogenic switch and extent of revascularization. *J. Clin. Invest* 116, 3277–3291. 10.1172/JCI29314. [PubMed: 17143334]
25. Qu S, Yang L, and Liu Z (2020). MicroRNA-194 reduces inflammatory response and human dermal microvascular endothelial cells permeability through suppression of TGF- β /SMAD pathway by inhibiting THBS1 in chronic idiopathic urticaria. *J. Cell. Biochem.* 121, 111–124. 10.1002/jcb.28941. [PubMed: 31190349]
26. Jiang D, Guo B, Lin F, Lin S, and Tao K (2020). miR-205 inhibits the development of hypertrophic scars by targeting THBS1. *Aging (Albany NY)* 12, 22046–22058. 10.18632/aging.104044. [PubMed: 33186919]
27. Sundaram P, Hultine S, Smith LM, Dews M, Fox JL, Biyashev D, Schelter JM, Huang Q, Cleary MA, Volpert OV, and Thomas-Tikhonenko A (2011). p53-responsive miR-194 inhibits thrombospondin-1 and promotes angiogenesis in colon cancers. *Cancer Res.* 71, 7490–7501. 10.1158/0008-5472.Can-11-1124. [PubMed: 22028325]
28. Filipowicz W, Bhattacharyya SN, and Sonenberg N (2008). Mechanisms of post-transcriptional regulation by microRNAs: are the answers in sight? *Nat. Rev. Genet* 9, 102–114. 10.1038/nrg2290. [PubMed: 18197166]
29. O'Brien J, Hayder H, Zayed Y, and Peng C (2018). C. Overview of MicroRNA biogenesis, mechanisms of actions, and circulation. *Front. Endocrinol.* 9, 402. 10.3389/fendo.2018.00402.

30. Ratajczak MZ (2017). Why are hematopoietic stem cells so ‘sexy’? on a search for developmental explanation. *Leukemia* 31, 1671–1677. 10.1038/leu.2017.148. [PubMed: 28502982]
31. Peng YJ, Yu H, Hao X, Dong W, Yin X, Lin M, Zheng J, and Zhou BO (2018). Luteinizing hormone signaling restricts hematopoietic stem cell expansion during puberty. *Embo j* 37, e98984. 10.15252/embj.201898984. [PubMed: 30037826]
32. Oguro H. (2019). The roles of cholesterol and its metabolites in normal and malignant hematopoiesis. *Front. Endocrinol* 10, 204. 10.3389/fendo.2019.00204.
33. Li Y, Huang B, Yang H, Kan S, Yao Y, Liu X, Pu S, He G, Khan TM, Qi G, et al. (2020). Latexin deficiency in mice up-regulates inflammation and aggravates colitis through HECTD1/Rps3/NF-kappaB pathway. *Sci. Rep.* 10, 9868. 10.1038/s41598-020-66789-x. [PubMed: 32555320]
34. Wan F, Weaver A, Gao X, Bern M, Hardwidge PR, and Lenardo MJ (2011). IKKbeta phosphorylation regulates RPS3 nuclear translocation and NF-kappaB function during infection with *Escherichia coli* strain O157:H7. *Nat. Immunol.* 12, 335–343. 10.1038/ni.2007. [PubMed: 21399639]
35. Liang Y, Van Zant G, and Szilvassy SJ (2005). Effects of aging on the homing and engraftment of murine hematopoietic stem and progenitor cells. *Blood* 106, 1479–1487. 10.1182/blood-2004-11-4282. [PubMed: 15827136]
36. Li B, and Dewey CN (2011). RSEM: accurate transcript quantification from RNA-Seq data with or without a reference genome. *BMC Bioinf.* 12, 323. 10.1186/1471-2105-12-323.
37. Robinson MD, McCarthy DJ, and Smyth GK (2010). edgeR: a Bioconductor package for differential expression analysis of digital gene expression data. *Bioinformatics* 26, 139–140. 10.1093/bio-informatics/btp616. [PubMed: 19910308]
38. Subramanian A, Tamayo P, Mootha VK, Mukherjee S, Ebert BL, Gillette MA, Paulovich A, Pomeroy SL, Golub TR, Lander ES, and Mesirov JP (2005). Gene set enrichment analysis: a knowledge-based approach for interpreting genome-wide expression profiles. *Proc. Natl. Acad. Sci. USA* 102, 15545–15550. 10.1073/pnas.0506580102. [PubMed: 16199517]

Highlights

- Latexin deletion does not have functional effects on HSCs and hematopoiesis in male mice
- Male-specific suppression of *Thbs1* underlies latexin-mediated hematopoiesis sex dimorphism
- Male-specific high expression of microRNA98-3p leads to *Thbs1* downregulation in male HSCs
- *Thbs1* reduction eliminates latexin's functional action on male HSCs and hematopoiesis

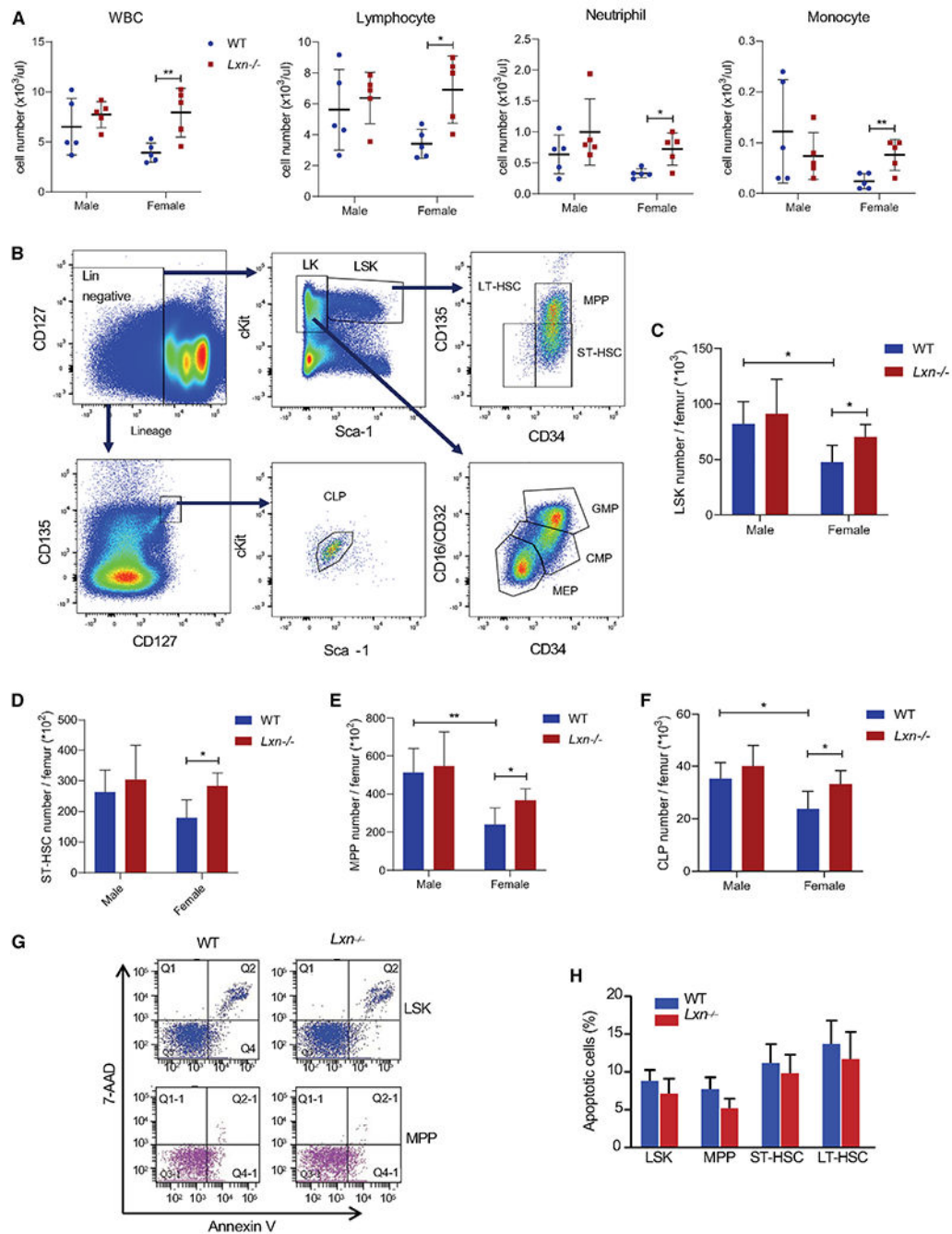


Figure 1. Latexin deletion *in vivo* does not affect the number of blood cells and BM HSPCs in male mice

(A) Differential blood cell counts of *Lxn*^{-/-} and WT male mice (n = 5 per group). The data were analyzed by two-tailed t test.

(B) Representative fluorescence-activated cell sorting (FACS) analysis of hematopoietic stem/progenitor cells. LSK cells are Lin⁻, ckit⁺, and sca-1⁺; LT HSC cells are Lin⁻, sca-1⁺, ckit⁺, CD34⁻, and CD135⁻; ST HSC cells are Lin⁻, sca-1⁺, ckit⁺, CD34⁺, and CD135⁻; MPP cells are Lin⁻, sca-1⁺, ckit⁺, CD34⁺, and CD135⁺; CLP cells are Lin⁻, sca-1^{med}, ckit^{med}, CD127⁺, and CD135⁺; MEP cells are Lin⁻, sca-1⁻, ckit⁺, CD34⁻, and

CD16/CD32⁻; CMP cells are Lin⁻, sca-1⁻, ckit⁺, CD34^{med}, and CD16/CD32^{med}; GMP cells are Lin⁻, sca-1⁻, ckit⁺, CD34⁺, and CD16/CD32⁺.

(C–F) The percentage of LSK cells (C), ST HSCs (D), MPP cells (E), and CLP cells (F) in one femur of *Lxn^{-/-}* and WT female and male mice.

(G) Representative flow cytometric analysis of annexin V⁺ and 7-AAD apoptotic LSK cells and MPP cells.

(H) Percentage of apoptotic cells in populations of LSK cells, MPP cells, LT HSCs, and ST HSCs from *Lxn^{-/-}* and WT male mice.

The data were analyzed by two-tailed t test and are shown as mean ± SD. **p < 0.01.

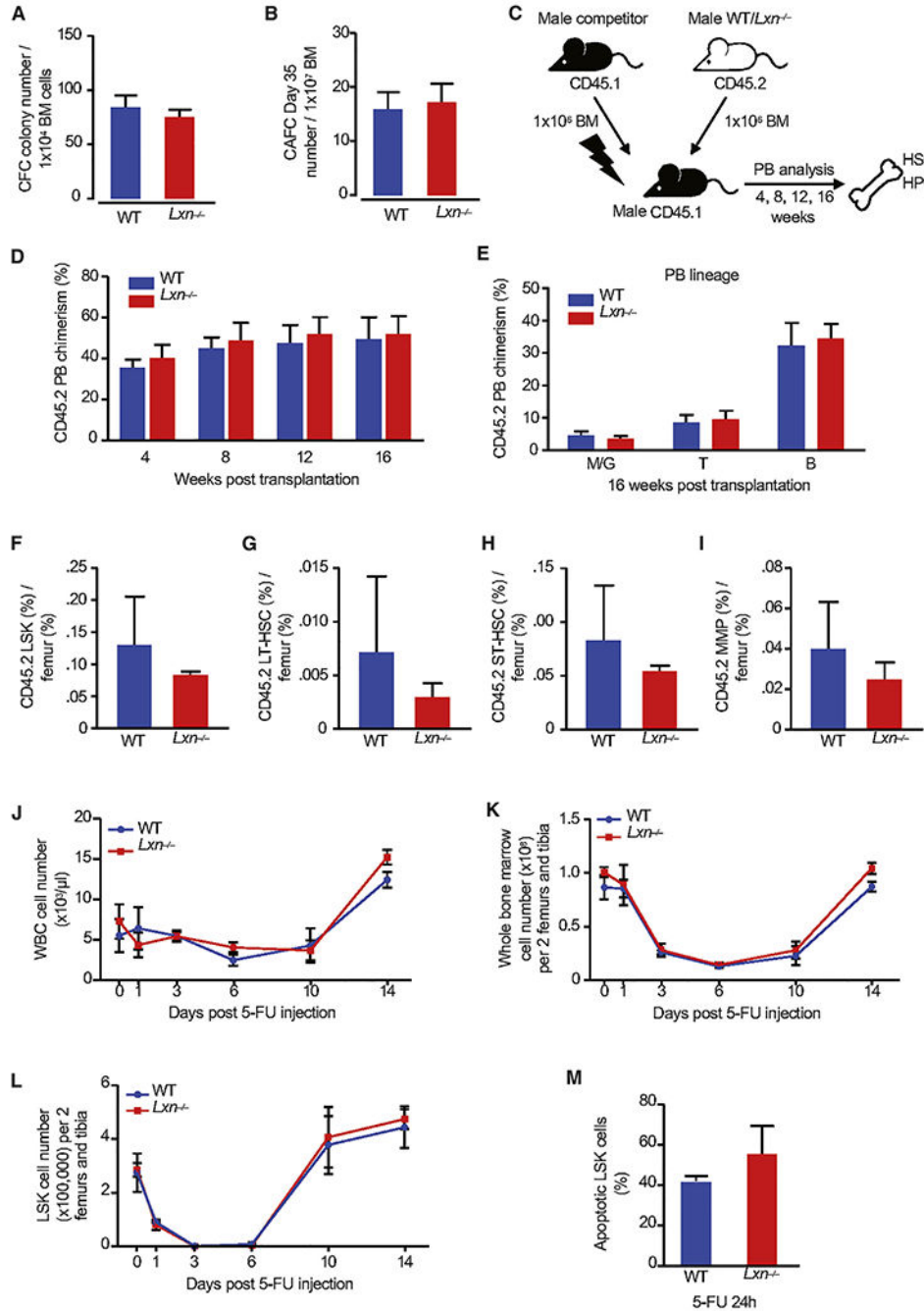


Figure 2. Deletion of latexin *in vivo* in male mice does not change the clonogenic and repopulation capacity of BM cells

(A) Absolute number of clones, defined by the cobblestone area-forming cell (CAFC) assay, assessed on day 35. Data presented are an average of six male mice for each group and analyzed by L-calc limiting dilution analysis software.

(B) Absolute number of clones, defined by the colony-forming cell (CFC) assay, assessed on day 14. Data presented are an average of three male mice for each group and were analyzed by two-tailed t test.

(C) Experimental scheme of competitive transplantation assay.

(D) Frequencies of $Lxn^{-/-}$ or WT donor (CD45.2)-derived leukocytes from peripheral blood (PB) of male recipient mice (CD45.1) at 4, 8, 12, and 16 weeks after transplantation.

(E) Frequencies of $Lxn^{-/-}$ or WT donor (CD45.2)-derived B cells, T cells, and myeloid cells at 16 weeks after transplantation obtained from the PB of male recipient mice (CD45.1). Data presented are the average of five male recipients for each group analyzed by two-way ANOVA.

(F–I) At 16 weeks after transplantation, the frequencies of $Lxn^{-/-}$ or WT donor (CD45.2)-derived cells, (F) the percentage of LSK cells, (G) LT HSCs, (H) ST HSCs, and (I) MPP cells per femur.

For (D)–(I), data presented are the average of five male recipients for each group.

(J) White blood cell counts in $Lxn^{-/-}$ and WT male mice at different time points post-5-FU-induced hematopoietic stress.

(K) Whole BM cell number recovery in $Lxn^{-/-}$ and WT male mice post-5-FU treatment.

(L) LSK cell recovery in $Lxn^{-/-}$ and WT male mice post-5-FU treatment.

(M) The percentage of apoptotic LSK cells 1 day after 5-FU injection. All parameters were monitored at days 0, 1, 3, 6, 10, and 14 post-5-FU treatment.

For (J)–(M), data presented are the average of three male mice for each group, and all data are shown as mean \pm SD and analyzed by two-tailed t test.

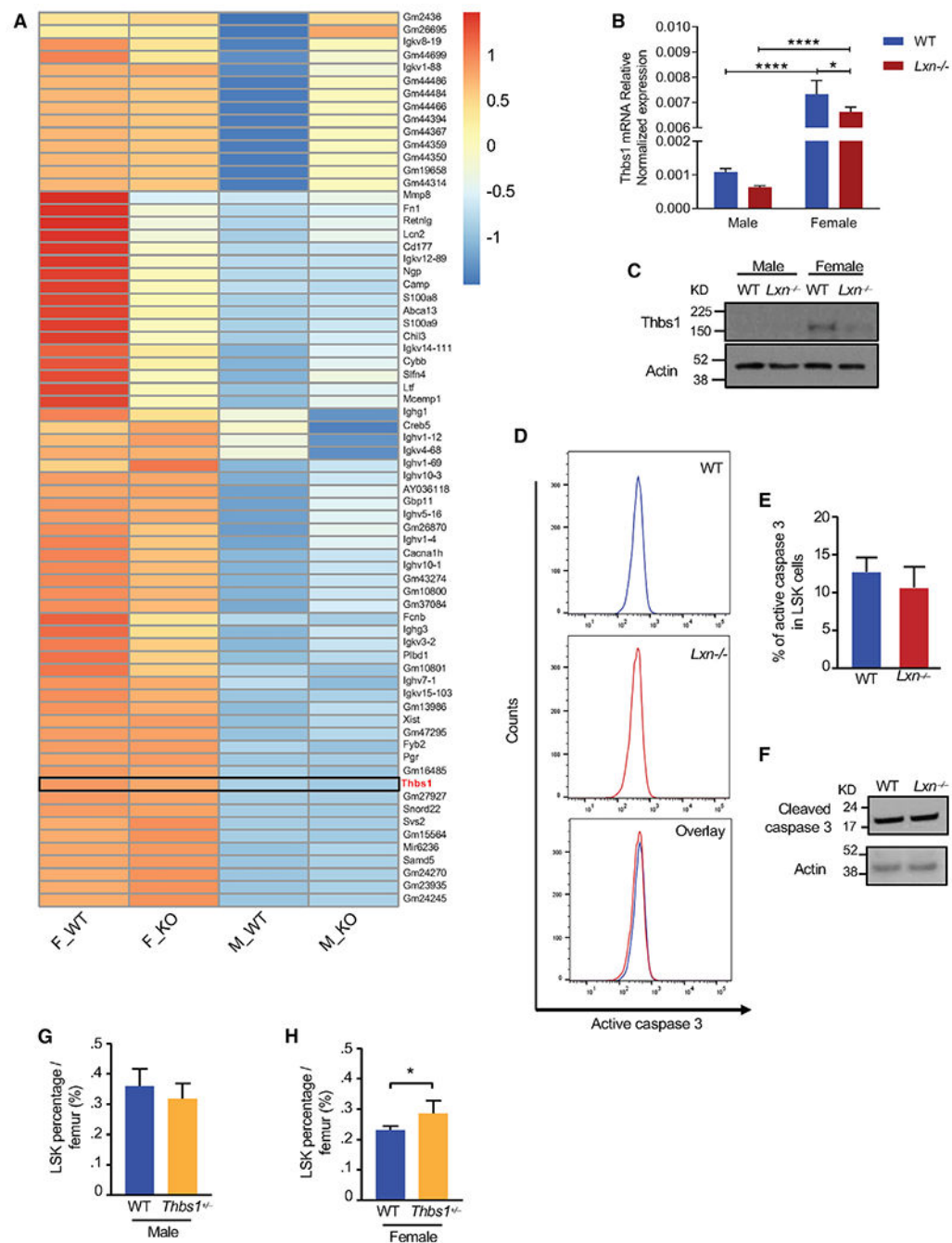


Figure 3. Thbs1 suppression in male HSCs contributes to latexin-mediated gender-specific regulation of hematopoiesis

(A) RNA-seq data of LSK cells from WT female, *Lxn*^{-/-} female, WT male, and *Lxn*^{-/-} male mice.

(B and C) The mRNA (B) and protein (C) levels of *Thbs1* in LSK cells of WT female, *Lxn*^{-/-} female, WT male, and *Lxn*^{-/-} male mice.

(D) Representative flow cytometric analysis of active caspase-3 protein in male WT and *Lxn*^{-/-} LSK cells.

(E) Frequency of LSK cells positive for active caspase-3.

(F) The protein level of cleaved caspase-3 protein in LSK cells of WT and *Lxn^{-/-}* male mice by western blot.

(G) Percentage of LSK cells in one femur of *Thbs1^{+/-}* and WT male mice.

(H) Percentage of LSK cells in one femur of *Thbs1^{+/-}* and WT female mice.

All data are shown as mean (n = 5–6) ± SD and were analyzed by two-tailed t test. *p < 0.05 and ****p < 0.0001.

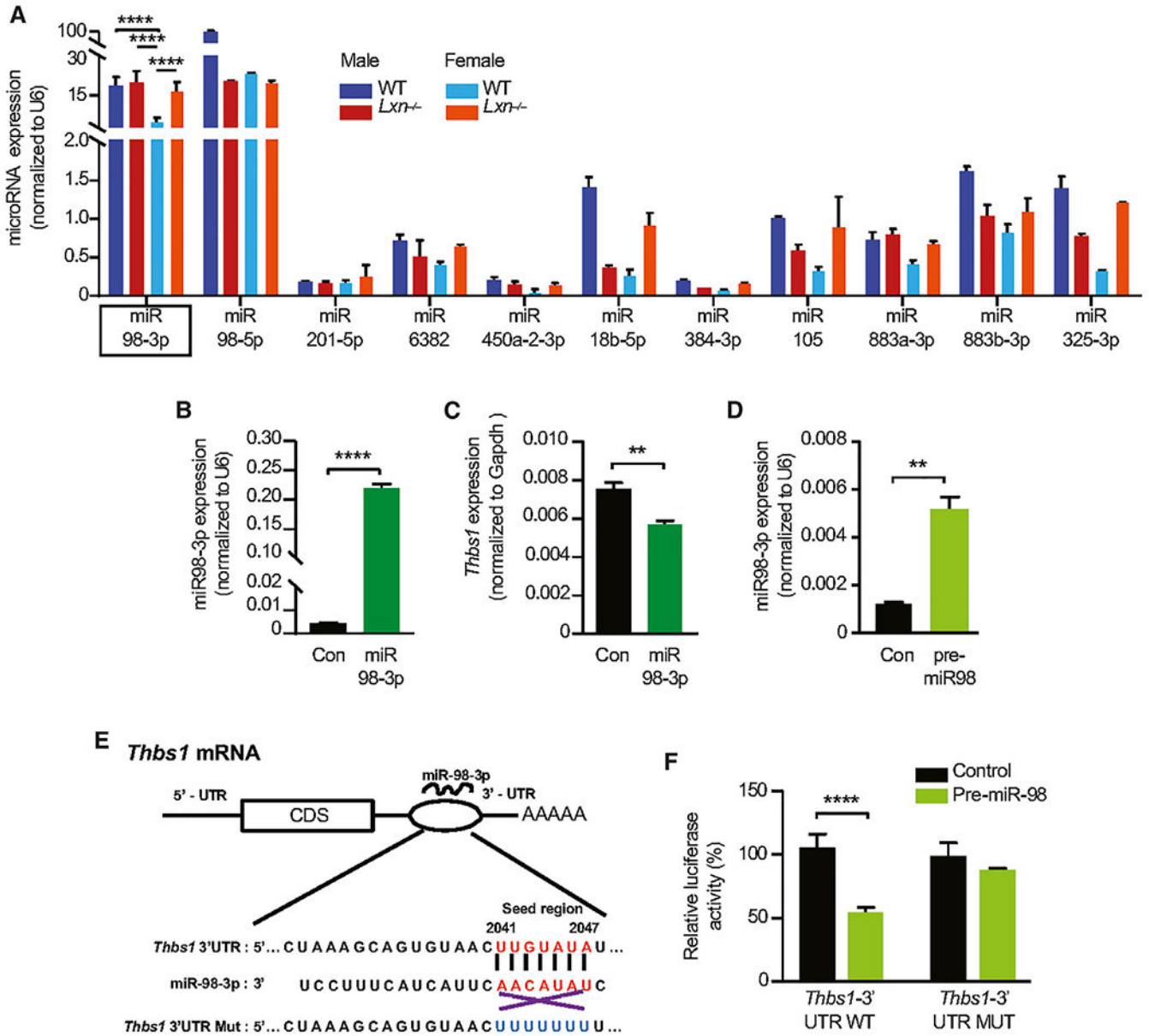


Figure 4. miR98-3p directly binds to *Thbs1* and inhibits its expression *in vitro*

(A) The expression of microRNA in LSK cells of WT female, *Lxn*^{-/-} female, WT male, and *Lxn*^{-/-} male mice by qPCR.

(B) The expression of miR98-3p in 3T3 cells transfected with control or miR98-3p mimics.

(C) The expression of *Thbs1* in 3T3 cells transfected with control or miR98-3p mimics.

(D) The expression of miR98-3p in 293T cells transfected with pcDNA3.1 control vector or pre-miR98.

(E) The scheme for potential binding of *Thbs1*-3' UTR and miR98-3p. The predicted binding (seed) region for miR98-3p spans from 2,041 to 2,047 of the *Thbs1*-3' UTR. The mutant was generated as the negative control (*Thbs1*-3' UTR-mut).

(F) The luciferase activity in 293T cells co-transfected with *Thbs1*-3' UTR-WT and empty vector control (pcDNA3.1) or pre-miR98 plasmid or with *Thbs1*-3' UTR-mut and empty vector control (pcDNA3.1) or pre-miR98 plasmid.

All data were derived from 2 independent experiments with 3 replicates from each experiment, are shown as mean \pm SD, and were analyzed by two-tailed t test. ** $p < 0.01$ and *** $p < 0.0001$.

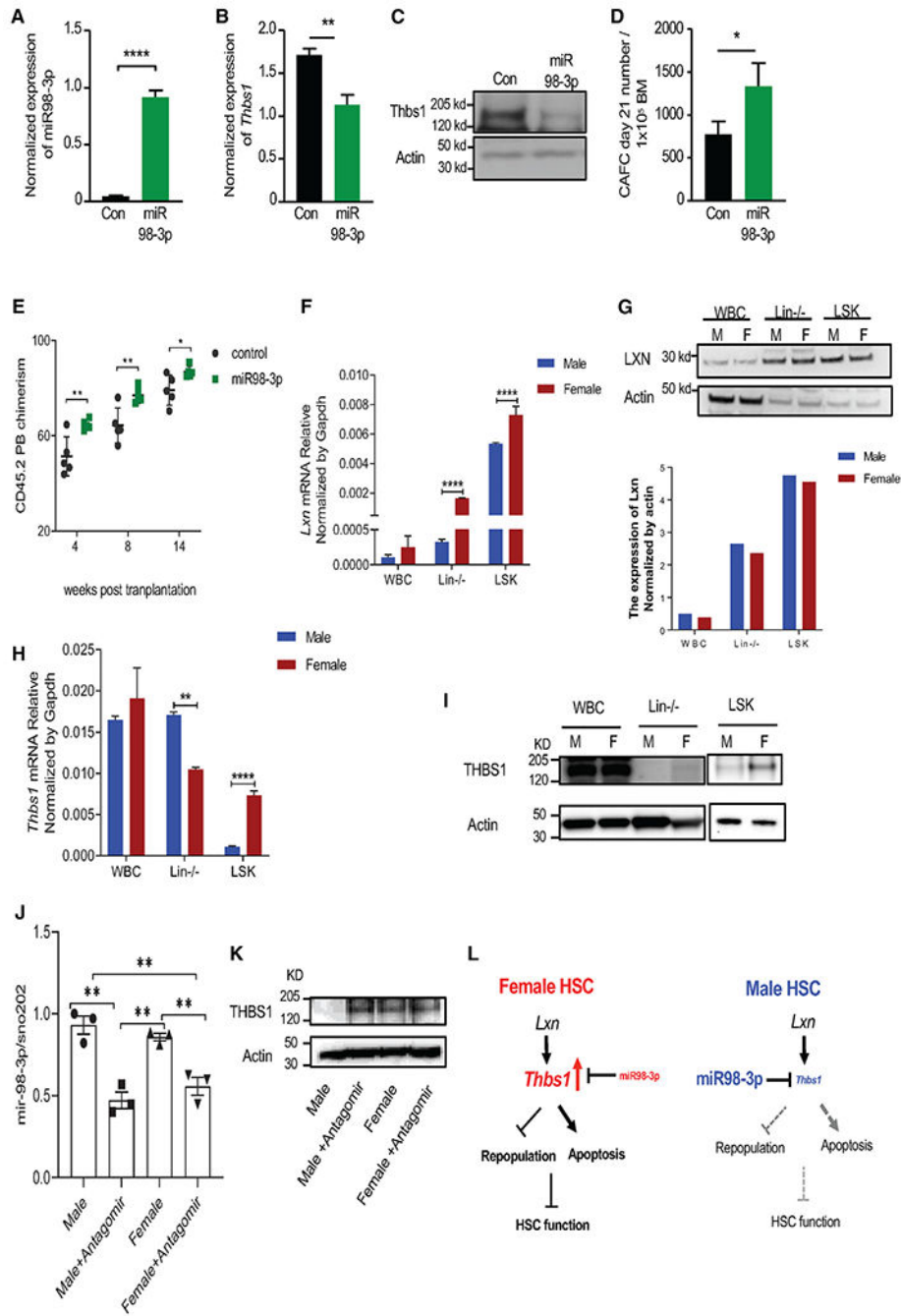


Figure 5. miR98-3p increases HSPC function by decreasing the *Thbs1* level in a sex-dependent manner

(A) The expression of miR98-3p in female LSK cells transfected with control or miR98-3p mimics was assessed by qPCR and quantified.

(B) The mRNA level of *Thbs1* in female LSK cells transfected with control or miR98-3p mimics was assessed by qPCR and quantified.

(C) The protein level of *Thbs1* in female LSK cells transfected with control or miR98-3p mimics was assessed by western blot.

(D) The absolute number of clones, defined by the CAFC assay, observed at day 21.

(E) Percentages of PB (CD45.2) chimerism in recipient mice (CD45.1, n = 5) that were transplanted with LSK cells treated with control or miR98-3p mimics at 4, 8, and 14 weeks after transplantation.

(F and G) *Lxn* mRNA expression (F) and Lxn protein expression (G) (top panel) and quantification (bottom panel) in WBCs, BM Lin⁻ cells, and HSPC-enriched LSK cells in male and female mice.

(H and I) *Thbs1* mRNA expression (H) and *Thbs1* protein expression (I) in WBCs, BM Lin⁻ cells, and HSPC-enriched LSK cells in male and female mice. Note: because *Thbs1* protein expression is very low in LSK cells, we used different exposure times in order for the band to show. We thus could not do the band quantification.

(J) miR-98-3p expression in male and female LSK cells treated with miR-98-3p antagonist or control.

(K) *Thbs1* protein expression in male and female LSK cells treated with miR-98-3p antagonist or control.

(L) The model for sex-/gender-specific regulation of HSCs and hematopoiesis by the *Lxn*, *mirR98-3p*, and *Thbs1* pathway. In female HSPCs, *Lxn* and low *mirR98-3p* expression upregulates *Thbs1* expression, which inhibits HSC repopulation and increases HSC apoptosis, thus impairing HSC function. In contrast, *mirR98-3p* expression is very high in male HSCs, leading to a very low level of *Thbs1*, which abrogates the functional effect of *Lxn* on male HSCs. Differential expression of sex-chromosome-specific *mirR98-3p* contributes to sex-dependent regulation of HSCs and hematopoiesis by *Lxn-Thbs1* signaling.

All the data are shown as mean \pm SD and were analyzed by two-tailed t test. *p < 0.05, **p < 0.01, and ****p < 0.0001.

KEY RESOURCES TABLE

REAGENT or RESOURCE	SOURCE	IDENTIFIER
Antibodies		
Gr-1	BD Biosciences	Cat# 553125; RRID: AB_394641
CD45R	BD Biosciences	Cat# 553086; RRID: AB_394615
CD11b	BD Biosciences	Cat# 553309; RRID: AB_394773
CD5	BD Biosciences	Cat# 553019; RRID: AB_394557
CD8a	BD Biosciences	Cat# 553029; RRID: AB_394566
Ter119	BD Biosciences	Cat# 553672; RRID: AB_394985
Streptavidin	BD Biosciences	Cat# 554063; RRID: AB_10054651
Sca-1	Invitrogen	Cat# 25-5981-82; RRID: AB_469669
eKit	BD Biosciences	Cat# 553356; RRID: AB_398536
CD135	BD Biosciences	Cat# 553842; RRID: AB_395079
CD34	BD Biosciences	Cat# 560238; RRID: AB_1645242
FcyR	BD Biosciences	Cat# 560540; RRID: AB_1645259
CD127	eBioscience	Cat# 48-1271-82; RRID: AB_2016698
CD45.1	BD Biosciences	Cat# 558701; RRID: AB_1645214
CD45.2	BD Biosciences	Cat# 561874; RRID: AB_10894189
CD90.2	eBiosciences	Cat# 25-0902-82; RRID: AB_469642
Mac-1	eBiosciences	Cat# 45-0112-82; RRID: AB_953558
Gr-1	BD Biosciences	Cat# 553128; RRID: AB_394644
B220	BD Biosciences	Cat# 552094; RRID: AB_394335
7-AAD	BD Biosciences	Cat# 559925
Thbs1	Santa Cruz	Cat# sc-59887
Lxn	Proteintech	Cat# 13056-1-AP
Cleaved caspase 3	Cell Signaling Technology	Cat# 9661S
Monoclonal Anti- β -Actin antibody	Sigma Aldrich	Cat# A2228-200UL
Chemicals, peptides, and recombinant proteins		
5-Fluorouracil (5-FU)	Sigma-Aldrich	Cat# F6627-5G

REAGENT or RESOURCE	SOURCE	IDENTIFIER
Mmu-miR-98-3p miRNA Mimic	Applied Biological Materials (abm) Inc	Cat# MCM03275
lipofectamine 3000	Invitrogen	Cat# L3000001
TaqMan Universal PCR Master Mix	Applied Biosystems	Cat# 4304437
Mmu-miR-98 miRNA Antagomir	Applied Biological Materials (abm) Inc	Cat# MNM03274
Mouse FMS-like tyrosine kinase-3 ligand	R & D systems	Cat# 427-FL-025/CF
Mouse IL-6	R & D systems	Cat# 406-ML
Mouse IL-3	R & D systems	Cat# 403-ML
Mouse stem cell factor	R & D systems	Cat# 455-MC
Critical commercial assays		
all-in-one miRNA qRT-PCR Detection Kits	GeneCopoeia	Cat# QP015; QP115
Dual-Glo Luciferase Assay System	Promega	Cat# E2920
mirVana miRNA Isolation Kit	Invitrogen	Cat# AM1561
RNeasy Micro kit	Qiagen	Cat# 74004
high-capacity cDNA reverse transcription kit	Applied Biosystems	Cat# 4368814
PE Annexin V Apoptosis Detection Kit I	BD Biosciences	Cat# 559763; RRID: AB_2869265
Deposited data		
Male WT LSK cells RNAseq raw and analyzed data	This paper	GSE213283
Female WT LSK cells RNAseq raw and analyzed data	This paper	GSE213283
Male <i>Lxn</i> ^{-/-} LSK cells RNAseq raw and analyzed data	This paper	GSE213283
Female <i>Lxn</i> ^{-/-} LSK cells RNAseq raw and analyzed data	This paper	GSE213283
Experimental models: Cell lines		
293T	ATCC	CRL-3216
3T3	ATCC	CRL-1658
Experimental models: Organisms/strains		
C57BL/6	Jackson Laboratory	N/A
B6.SJL/BoyJ (CD45.1)	Jackson Laboratory	N/A
<i>Lxn</i> constitutive knockout mice (<i>Lxn</i> ^{-/-})	Liu et al. ¹⁵	N/A
Oligonucleotides		
miR98-3p: AGCGAGGCCTATACAACCTACTACT	This paper	N/A
miR98-5p: AAGCGACCTGAGGTAGTAAGTTGTA	This paper	N/A
U6: CTCGCTTCGGCAGCACA	This paper	N/A
miR201-5p: AACCGTACTCAGTAAGGCATTG	This paper	N/A
miR-6382: AACAGTGTGGAATGTAAAGAGAGCA	This paper	N/A

REAGENT or RESOURCE	SOURCE	IDENTIFIER
miR-450a-2-3p: AACAAATATTGGGGATGCTTTGCATT	This paper	N/A
miR-18b-5p: AACACGCTAAGGTGCATCTAGTG	This paper	N/A
miR-384-3p: AACGGCATTCTAGAAATTGTTTCCAC	This paper	N/A
miR-105: AACAGTGCCAAGTGCTCAGATG	This paper	N/A
miR-883a-3p: AACAGATAACTGCAACAGCTCTCAG	This paper	N/A
miR-883b-3p: AACCACTTAACTGCAACATCTCTCA	This paper	N/A
miR-325-3p: AACCATGTTTATTGAGCACCTCCT	This paper	N/A
Pre-miR98 forward primer (5' to 3'): CCGGATCCCATTACATACATATACTTCTCATTCCTTCT	This paper	N/A
Pre-miR98 reverse primer: CGGAATTCGATGAACCAACATGCCTTGC	This paper	N/A
pGL3-Thbs1-3' UTR-wt forward primer: GCTCTAGAGCCATTTTATCCATTTTACATTTCTAAAGCAGTGTAAGTTGTATAT	This paper	N/A
pGL3-Thbs1-3' UTR-wt reverse primer: GCTCTAGAGCTACATAAGAAACAGTAAATATACAAGTTACTGCTTTAGAATGT	This paper	N/A
pGL3-Thbs1-3' UTR-mut forward primer: GCTCTAGAGCCATTTTATCCATTTTACATTTCTAAAGCAGTGTAAGTTTTTTTT	This paper	N/A
pGL3-Thbs1-3' UTR-mut reverse primer: GCTCTAGAGCTACATAAGAAACAGTAAAAAAAAGTTACTGCTTTAGAATGT	This paper	N/A
<i>Thbs1</i> CpG-260bp forward primer: TTTTAGGTGGTTTTTAAAGAAAGTAT	This paper	N/A
<i>Thbs1</i> CpG-260bp reverse primer: TAAAAAACAAAAACAAAAAAA	This paper	N/A
<i>Thbs1</i> CpG-147bp forward primer: TTTAGTTAAGTTAGTTATTGTTTGGAGTTA	This paper	N/A
<i>Thbs1</i> CpG-147bp reverse primer: CTAATCATCTACAACCTAAAACCTTTAAAAT	This paper	N/A
Recombinant DNA		
pre-miR98 plasmid	This paper	N/A
pGL3- <i>Thbs1</i> -3' UTR-wt plasmid	This paper	N/A
pGL3- <i>Thbs1</i> -3' UTR-mut plasmid	This paper	N/A
Software and algorithms		
GraphPad Prism	GraphPad Prism	v7 - v9
Cytometers BD LSRII	BD	N/A
L-CaLc limiting dilution analysis software	STEMCELL Technologies	N/A
ImageJ	N/A	N/A